Lasers in Medical Science (2026) 41:176
https://doi.org/10.1007/s10103-026-04959-5

RESEARCH

Cadaveric analysis of periosteal temperature response across skin types in facial tissues using a multi-wavelength diode laser

Kyu-Ho Yi[1] · Yerin Park[2] · Hugues Cartier[3] · Sebastien Garson[4] · Benjamin Ascher[5]

Received: 6 April 2026 / Accepted: 13 July 2026
© The Author(s) 2026

Abstract

Energy-based devices are often applied to the midface using uniform treatment parameters despite interindividual variability in facial anatomy and skin pigmentation. For bulk-heating technologies, clinical relevance depends not only on superficial heating but also on the timing and magnitude of temperature rise at deeper tissue planes, as periosteal thermal exposure in the malar cheek may influence procedural safety and discomfort. This study aimed to quantify time to periosteal temperature rise in the malar cheek and to compare this parameter between Fitzpatrick skin types I–II and III–IV. This cadaveric study was conducted using four human hemifaces representing Fitzpatrick skin types I–IV, grouped into I–II and III–IV. A multi-wavelength diode laser was applied to a malar cheek region using a stacking technique. Periosteal temperature at the zygomatic bone was measured with a thermocouple. Time to periosteal temperature rise was defined as the elapsed time from laser activation to the first sustained periosteal temperature increase of ≥0.5 °C above baseline. Mean time to periosteal temperature rise was longer in Fitzpatrick I–II specimens (6.4 ± 0.5 s) than in Fitzpatrick III–IV specimens (4.7 ± 0.4 s). Peak temperatures were higher in Fitzpatrick III–IV (68–71 °C) than in Fitzpatrick I–II (58–62 °C). Fitzpatrick III–IV specimens showed earlier periosteal temperature rise and higher peak periosteal temperatures under identical delivery settings, supporting skin type–dependent differences in deep thermal response during stacking delivery of a multi-wavelength diode laser.

Keywords Multi-wavelength diode laser · Periosteal temperature response · Fitzpatrick skin type · Cadaveric study · Malar cheek

Introduction

Thermal energy–based technologies, including lasers, radiofrequency, and microfocused ultrasound, constitute a central component of contemporary facial rejuvenation and contouring strategies. Controlled thermal exposure has been shown to induce collagen remodeling, tissue contraction, and, in selected contexts, modification of subcutaneous adipose tissue [1, 3, 5]. Accordingly, most clinical protocols have traditionally emphasized surface safety and visible aesthetic outcomes.

In routine clinical practice, however, uniform energy parameters are frequently applied without fully accounting for inter-individual differences in skin pigmentation and facial tissue architecture. As a result, thermal behavior beyond the superficial layers—particularly the timing and extent of temperature rise at deeper anatomical planes—has often been inferred rather than directly characterized. In the malar cheek, deep-plane heating may influence both

✉ Kyu-Ho Yi
kyuho90@daum.net

Yerin Park
iisabelle559@gmail.com

Hugues Cartier
h.cartier@imcas.com

Sebastien Garson
s.garson@imcas.com

Benjamin Ascher
doctorbenjaminascher@gmail.com

1 You and I Clinic, Seoul, Republic of Korea

2 Medical Research, Wonju, Republic of Korea

3 Centre Médical Saint Jean, Arras, France

4 Cabinet Médical, Senlis, France

5 SIBUS-In, Paris, France

Published online: 03 August 2026

procedural tolerability and safety. Patients commonly localize treatment-related discomfort to areas overlying osseous prominences, suggesting that periosteal warming may represent a clinically relevant contributor to procedural sensation [4, 8].

From a biophysical perspective, tissue response to thermal energy cannot be inferred solely from surface parameters. Subsurface temperature behavior reflects the combined effects of optical absorption, tissue-specific scattering, local anatomy, and conductive heat transfer [11, 13, 16]. Melanin content can modify the initial spatial distribution of absorbed optical energy, particularly at shorter near-infrared wavelengths, thereby modifying both the magnitude and spatial distribution of heat generation. In addition, the malar cheek demonstrates anatomical variability in dermal thickness, subcutaneous tissue composition, and fibrous septal organization, all of which may influence internal temperature profiles during and after irradiation. Prior studies of thermal dynamics consistently demonstrate that identical surface energy delivery can result in substantially different internal temperature patterns depending on tissue composition and anatomical structure.

Despite these considerations, prior investigations of facial thermal technologies have largely focused on clinical efficacy or surface-level safety endpoints [6, 17]. Direct anatomical studies evaluating deep facial temperature response during fixed-spot energy delivery remain limited, particularly for techniques that rely on repeated energy deposition at a single location. Time-based evaluation of periosteal temperature response may therefore provide clinically relevant information that is not captured by surface temperature measurements alone.

Accordingly, the present study examines the time required for periosteal temperature rise to occur of the malar cheek during stacking delivery using a multi-wavelength diode laser. By quantifying this periosteal temperature-response interval, this cadaveric anatomical investigation compares deep thermal response timing between Fitzpatrick skin type groups under standardized irradiation conditions.

Methods & materials

Study design and specimens

This was an anatomical cadaveric study designed to characterize periosteal temperature response timing in the malar cheek. Four cadaveric hemifaces representing Fitzpatrick skin types I, II, III, and IV were included. For analysis, specimens were grouped as Fitzpatrick I–II ($n=2$ hemifaces) and Fitzpatrick III–IV ($n=2$ hemifaces). All specimens had intact facial skin without gross scarring, prior surgical alteration, or dermatologic disease that could materially affect heat conduction.

Each hemiface underwent three repeated measurements at the same region of interest, with thermocouple repositioning and reconfirmation of periosteal contact before each measurement. Mean values per hemiface were calculated for group-level comparisons.

All cadaveric specimens were obtained from the body donation program. Specimens were handled in accordance with institutional policies and applicable regulations, and donors had provided informed consent for the use of their bodies for medical education and research prior to donation. The study protocol was approved by the Public Institutional Bioethics Committee designated by the Ministry of Health and Welfare, Republic of Korea (IRB No. P01-202607-01-121) and was conducted in accordance with the Declaration of Helsinki.

Region of interest

The analysis was restricted to the malar cheek (malar eminence/zygomatic region). A standardized square region of interest measuring approximately 4 × 4 cm was marked on each hemiface. Only one ROI per hemiface was treated to avoid cross-heating effects.

Device and energy delivery

Laser irradiation was performed using a multi-wavelength diode laser system (Fortra, Classys Inc., Seoul, South Korea), which simultaneously emits four wavelengths (755, 808, 940, and 1064 nm) through one integrated 4D Multi handpiece and is designed to deliver non-ablative bulk thermal energy across superficial to deep tissue layers.

All experiments were conducted using the INTENSIVE (stacking) mode to intentionally accumulate thermal energy at a fixed location. Sapphire contact cooling was applied at −3 °C throughout irradiation to stabilize epidermal temperature. Laser parameters were standardized to a fluence of 0.6 J/cm² with eight consecutive stacks delivered at a pulse repetition rate of 1 Hz and a pulse interval of 0.5 s, resulting in a total stacking duration of 4.0 s per region of interest. During irradiation, the handpiece was maintained perpendicular to the skin surface with continuous full contact and consistent manual pressure to ensure uniform energy delivery.

Temperature measurement

A fine K-type thermocouple sensor (diameter 0.5 mm; response time < 0.3 s) was positioned at the periosteal plane of the zygomatic bone via a percutaneous insertion track. The sensor was advanced until firm periosteal contact was confirmed by tactile resistance. Insertion depth was recorded for each specimen according to specimen thickness and local anatomy. Temperature signals were recorded at a sampling rate of 10 Hz during irradiation and the immediate post-irradiation period.

Primary endpoint: time to periosteal temperature rise

The primary endpoint was time to periosteal temperature rise (seconds), defined as the elapsed time from laser activation to the first sustained periosteal temperature increase ≥ 0.5 °C above baseline persisting for at least 2 consecutive seconds (≥ 20 data points). This criterion was chosen to minimize noise-related artifacts and to capture a reproducible deep-plane thermal response threshold.

Secondary observations

Thermal patterns were assessed using infrared thermography to document temperature distribution within the treated malar cheek region following irradiation. Infrared imaging was performed after surgical exposure of the malar tissues, allowing visualization of thermal distribution within exposed facial tissues rather than intact skin surface alone.

Statistical approach

Mean times to periosteal temperature rise were calculated for each Fitzpatrick group. Between-group differences were assessed using a two-tailed t-test, with data presented as descriptive comparative findings centered on the pre-specified primary endpoint.

Results

Time to Periosteal Temperature Rise by Skin Type

Under identical stacking parameters, time to periosteal temperature rise differed between Fitzpatrick skin type groups. Fitzpatrick I–II specimens demonstrated a mean time to periosteal temperature rise of 6.4 ± 0.5 s, whereas Fitzpatrick III–IV specimens demonstrated a mean time of 4.7 ± 0.4 s. This between-group difference reached statistical significance despite the limited sample size.

Depth recording and procedural consistency

Insertion depth to the periosteal plane varied among specimens (4.5–5.0 cm). The same ROI dimensions, contact cooling temperature, stacking parameters, and delivery technique were used across all measurements.

Secondary observations: peak thermal exposure

Infrared thermography confirmed rapid temperature elevation within the malar tissues during stacking delivery. Under identical irradiation parameters, Fitzpatrick III–IV specimens consistently reached higher peak thermal exposure than Fitzpatrick I–II specimens. Peak tissue temperatures in Fitzpatrick III–IV specimens approached approximately 68–71 °C, whereas peak temperatures in Fitzpatrick I–II specimens remained lower, generally in the range of 58–62 °C, as demonstrated by infrared thermographic imaging (Fig. 1). Thermal monitoring further demonstrated that higher peak thermal exposure in

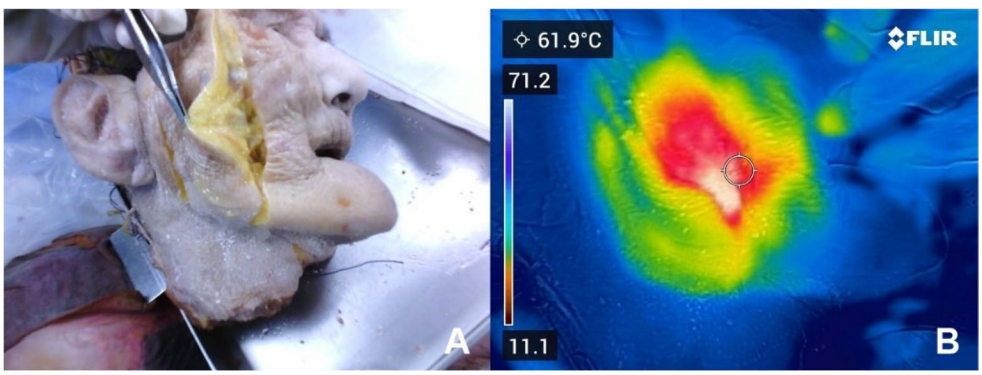

Fig. 1 Infrared thermographic image of thermal distribution in exposed malar tissues in a Fitzpatrick I–II specimen. Gross anatomical view of the exposed malar region (**A**) and corresponding infrared thermographic image (**B**) following irradiation. Warmer color gradients indicate areas of higher thermal accumulation, and the peak temperature reached 61.9 °C

Fitzpatrick III–IV specimens was accompanied by more sustained temperature elevation during the stacking phase.

Discussion

Multi-wavelength diode lasers and bulk heating dynamics

Diode lasers generate tissue heating through wavelength-dependent absorption by endogenous chromophores, including melanin, water, and lipid components. Shorter near-infrared wavelengths, such as 755 nm and 808 nm, exhibit higher melanin absorption and preferentially deposit energy within the epidermis and superficial dermis, whereas longer wavelengths, including 940 nm and 1064 nm, penetrate more deeply and are absorbed predominantly by water- and lipid-rich tissues in the deeper dermal and subcutaneous layers (Fig. 2). Multi-wavelength diode laser systems are designed to leverage these complementary absorption profiles by delivering all four wavelengths (755, 808, 940, and 1064 nm) simultaneously through one integrated 4D Multi handpiece [9, 10, 12].

The theoretical advantage of this approach lies in its ability to generate overlapping thermal effects across multiple tissue depths during a single irradiation sequence, thereby producing bulk heating rather than a narrowly confined thermal zone [2, 16]. Compared with single-wavelength systems, simultaneous multi-wavelength delivery may create a broader vertical distribution of deposited heat across superficial and deeper tissue layers, particularly when combined with fixed-spot stacking techniques that intentionally minimize lateral energy dispersion.

Despite this rationale, prior investigations of diode laser–based facial treatments have largely focused on clinical feasibility, safety, and aesthetic outcomes [6, 7, 17]. Few studies have examined how simultaneous delivery of shorter (755–808 nm) and longer (940–1064 nm) near-infrared wavelengths interacts with anatomically heterogeneous facial tissues to shape deep temperature response or how delivery technique influences the timing of deep-plane thermal exposure. As a result, the anatomical basis for periosteal temperature response during multi-wavelength diode laser treatment remains insufficiently characterized.

Periosteal temperature response across skin types

The central finding of the present study is that, under identical stacking parameters, Fitzpatrick III–IV specimens exhibited significantly shorter times to periosteal temperature rise than Fitzpatrick I–II specimens. This difference indicates that, despite standardized external delivery conditions, deep thermal response timing can differ across skin type groups.

Fitzpatrick skin types III–IV are characterized by higher epidermal and superficial dermal melanin content compared with types I–II. Melanin is a strong optical absorber in the near-infrared spectrum, particularly at shorter wavelengths such as 755 and 808 nm [10, 12]. Under multi-wavelength irradiation, this increased melanin concentration results in greater photon absorption within the superficial skin layers, leading to more efficient conversion of optical energy into thermal energy within superficial tissue layers. In the context of stacking delivery, repeated energy deposition at a fixed location further amplifies this effect, creating a larger and more rapidly established superficial thermal reservoir.

The present finding of shorter time to periosteal temperature rise in Fitzpatrick III–IV specimens is consistent with this mechanism. Greater initial heat generation in the superficial layers may contribute to a steeper local temperature profile and to earlier measurable temperature rise at deeper

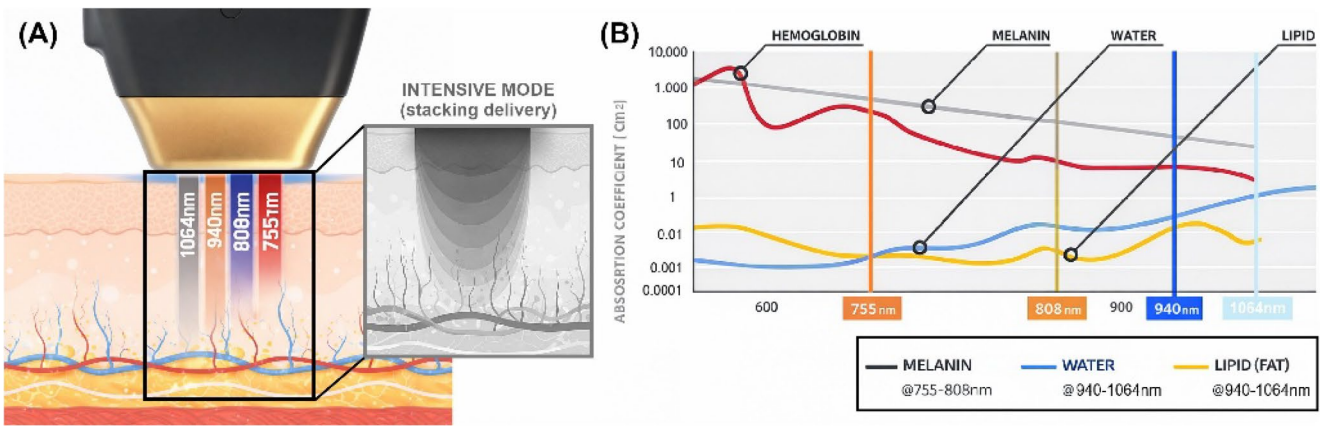

Fig. 2 Wavelength-dependent absorption and penetration profiles of multi-wavelength diode laser irradiation. Illustration of relative penetration depths of 755, 808, 940, and 1064 nm wavelengths within cutaneous tissues (**A**) and corresponding absorption spectra of major endogenous chromophores, including melanin, water, hemoglobin, and lipid (**B**)

planes during stacking delivery. Experimental studies of thermal dynamics have demonstrated that, under otherwise identical irradiation parameters, differences in surface heat generation can alter internal temperature profiles and deep tissue temperature response [2, 11, 13]. In the malar cheek—where the dermis, subcutaneous tissue, and periosteum are separated by a relatively short anatomical distance—these differences in superficial heat buildup and subsequent tissue temperature distribution are likely to translate into earlier periosteal temperature elevation.

In addition to differences in absorption, darker skin types exhibit lower optical reflectance and altered scattering behavior, which reduce outward energy loss and favor heat retention within the tissue matrix [9, 16]. These properties prolong the persistence of generated heat and facilitate its downward propagation. When combined with stacking delivery, which intentionally limits lateral dispersion, the net effect is a more efficient vertical transmission of thermal energy toward deep anatomical boundaries.

Clinical relevance of time-to-periosteum

The periosteal plane constitutes a biologically and clinically meaningful deep boundary in the malar cheek. In clinical practice, patients frequently localize heightened discomfort to areas overlying osseous prominences during thermal energy–based procedures, suggesting that periosteal warming may represent a relevant contributor to procedural sensation [14, 15]. Although cadaveric models cannot reproduce pain perception or active thermoregulation, time to periosteal temperature rise provides a pragmatic surrogate for evaluating deep-plane thermal exposure.

Within this framework, the present finding that Fitzpatrick III–IV specimens demonstrated both shorter times to periosteal temperature rise and higher peak thermal exposure than Fitzpatrick I–II specimens under identical delivery conditions is clinically informative, indicating that deep-plane thermal exposure may occur earlier and more intensely in darker skin types even when surface-level parameters are held constant; such differences in deep thermal response timing may help explain inter-individual variability in treatment sensation and tolerance, particularly in anatomically constrained regions such as the malar cheek. A key limitation of cadaveric thermal studies is the absence of perfusion and active thermoregulation, which may influence absolute temperature profiles and cooling kinetics in vivo; nevertheless, focusing on periosteal temperature rise under standardized delivery provides an anatomical framework for understanding how stacking-based bulk heating can generate measurable deep-plane thermal exposure in the cheek. To extend these anatomical observations to a clinical context, representative clinical photographs acquired 1 month after midface treatment with the same multi-wavelength diode laser system are shown (Fig. 3).

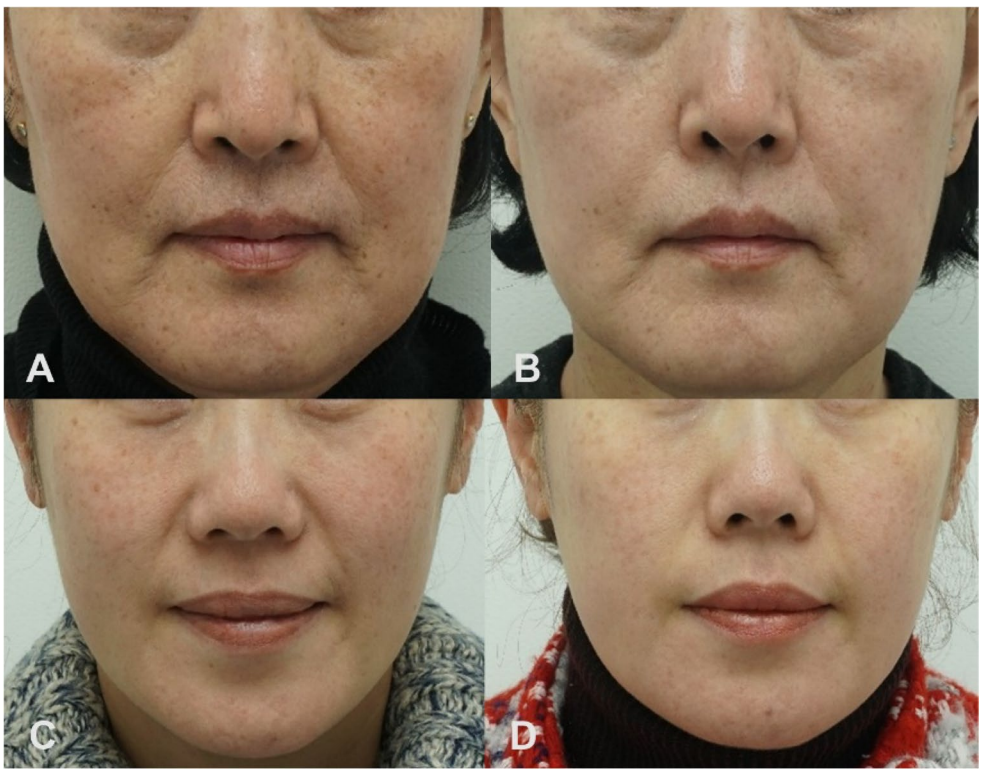

Fig. 3 Representative clinical photographs obtained before (**A**, **C**) and 1 month after (**B**, **D**) midface treatment with a multi-wavelength diode laser. At 1-month, qualitative improvement in malar contour with apparent softening of the nasolabial fold and a smoother midfacial appearance is observed

Qualitative improvement in malar contour with apparent elevation of the midface and softening of the nasolabial fold is observed, resulting in a smoother overall facial appearance. These appearance changes are compatible with non-ablative bulk heating across superficial-to-deep tissue planes and subsequent collagen remodeling and tissue contraction, and the cadaveric findings provide an anatomical context for how stacking delivery can be associated with measurable deep-plane thermal exposure in the malar cheek. Prospective studies incorporating standardized photography and objective outcome measures will further define therapeutic efficacy and safety.

Limitations

This work is limited by its cadaveric design and small sample typical of anatomical thermal studies. Cadaver tissues lack perfusion and active thermoregulation, so absolute temperature profiles may not replicate in vivo behavior. However, the comparative nature of the primary endpoint (time to detectable periosteal rise under identical conditions) still provides insight into differences in deep thermal response timing across skin types. In addition, the representative clinical photographs were included to provide translational context. These images were not obtained within a prospective efficacy protocol and were not quantitatively analyzed; therefore, they should be considered illustrative rather than definitive with respect to clinical effectiveness or safety. Further studies with larger specimen numbers and complementary measurement approaches including in vivo modeling, controlled clinical thermography, and more granular depth mapping are warranted.

Implications for future protocol development

The findings of this study support a shift away from strictly uniform facial laser protocols toward more individualized strategies that consider both delivery technique and patient-specific tissue characteristics. In the context of fixed-spot stacking over the malar cheek, clinicians may need to adjust dwell time, stack count, or cooling strategies according to skin type to mitigate unintended deep-plane heating while preserving desired superficial or subcutaneous effects.

By establishing time to periosteal temperature rise as a practical and clinically relevant deep-plane metric, this anatomical investigation provides a framework for interpreting variability in deep thermal response and lays the groundwork for future in vivo and clinical studies aimed at optimizing safety and efficacy in multi-wavelength diode laser treatments.

Conclusion

In a cadaveric malar cheek model using a multi-wavelength diode laser with contact cooling and stacking delivery, the time to periosteal temperature rise differed by skin type group. Fitzpatrick III–IV specimens demonstrated earlier periosteal temperature rise (mean 4.7 s) than Fitzpatrick I–II specimens (mean 6.4 s), with a statistically significant between-group difference. Time to periosteal temperature rise provides a practical deep-plane metric that may help inform individualized protocol design when fixed-spot stacking techniques are used on the cheek.

Authors' contributions All authors have reviewed and approved the article for submission. Conceptualization: Kyu-Ho YiMethodology: Kyu-Ho Yi, Yerin Park. Investigation: Yerin Park, Hugues Cartier, Sebastien Garson, Benjamin Ascher. Data curation: Yerin Park. Formal analysis: Kyu-Ho Yi, Yerin Park. Writing—original draft preparation: Yerin Park. Writing—review and editing: Kyu-Ho Yi, Hugues Cartier, Sebastien Garson, Benjamin Ascher. Visualization: Yerin Park. Supervision: Kyu-Ho Yi.

Funding This research received no specific grant from any funding agency.

Data availability The data that support the findings of this study are available on request from the corresponding author. The data are not publicly available due to privacy or ethical restrictions.

Declarations

Ethical approval The study protocol was approved by the Public Institutional Bioethics Committee designated by the Ministry of Health and Welfare, Republic of Korea (IRB No. P01-202607-01-121) and was conducted in accordance with the Declaration of Helsinki.

Consent to participate Donors had provided informed consent prior to donation for the use of their bodies in medical education and research.

Consent to publish Written informed consent for publication of clinical images was obtained from the donors.

Conflict of interest The authors declare no potential conflicts of interest with respect to the research, authorship, and/or publication of this article.

Competing interests The authors declare no competing interests.

Clinical trial number Not applicable.

Open Access This article is licensed under a Creative Commons Attribution-NonCommercial-NoDerivatives 4.0 International License, which permits any non-commercial use, sharing, distribution and reproduction in any medium or format, as long as you give appropriate credit to the original author(s) and the source, provide a link to the Creative Commons licence, and indicate if you modified the licensed material. You do not have permission under this licence to share adapted material derived from this article or parts of it. The images or

other third party material in this article are included in the article's Creative Commons licence, unless indicated otherwise in a credit line to the material. If material is not included in the article's Creative Commons licence and your intended use is not permitted by statutory regulation or exceeds the permitted use, you will need to obtain permission directly from the copyright holder. To view a copy of this licence, visit http://creativecommons.org/licenses/by-nc-nd/4.0/.

References

1. Abraham MT, Chiang SK, Keller GS, Rawnsley JD, Blackwell KE, Elashoff DA (2004) Clinical evaluation of non-ablative radiofrequency facial rejuvenation. J Cosmet Laser Ther Nov 6(3):136–144. https://doi.org/10.1080/14764170410023802
2. Asadi S, Bianchi L, De Landro M, Korganbayev S, Schena E, Saccomandi P (2021) Laser-induced optothermal response of gold nanoparticles: From a physical viewpoint to cancer treatment application. J Biophotonics Feb 14(2):e202000161. https://doi.org/10.1002/jbio.202000161
3. Atiyeh BS, Dibo SA (2009) Nonsurgical nonablative treatment of aging skin: radiofrequency technologies between aggressive marketing and evidence-based efficacy. Aesthetic Plast Surg May 33(3):283–294. https://doi.org/10.1007/s00266-009-9361-9
4. Austin GK, Struble SL, Quatela VC (2022) Evaluating the effectiveness and safety of radiofrequency for face and neck rejuvenation: A systematic review. Lasers Surg Med 54(1):27–45. https://doi.org/10.1002/lsm.23506
5. Ayatollahi A, Gholami J, Saberi M, Hosseini H, Firooz A (2020) Systematic review and meta-analysis of safety and efficacy of high-intensity focused ultrasound (HIFU) for face and neck rejuvenation. Lasers Med Sci Jul 35(5):1007–1024. https://doi.org/10.1007/s10103-020-02957-9
6. Doshi SN, Alster TS (2005) Combination radiofrequency and diode laser for treatment of facial rhytides and skin laxity. J Cosmet Laser Ther Mar 7(1):11–15. https://doi.org/10.1080/14764170410003075
7. Katz B, Doherty S (2018) Safety and Efficacy of a Noninvasive 1,060-nm Diode Laser for Fat Reduction of the Flanks. Dermatol Surg Mar 44(3):388–396. https://doi.org/10.1097/DSS.0000000000001298
8. Kumar V, Jain A, Vadera S, Shome D, Kapoor R (2023) Effectiveness of HIFU Therapy for Nonsurgical Facial and Body Contouring: A Systematic Review of Prospective and Experimental Studies. Plast Reconstr Surg Mar 1(3):533–544. https://doi.org/10.1097/prs.0000000000009912
9. Lowry KM, Beavers EM (1994) Thermal stability of sodium hyaluronate in aqueous solution. J Biomed Mater Res Oct 28(10):1239–1244. https://doi.org/10.1002/jbm.820281014
10. Majdabadi A, Abazari M (2014) Analysis of Laser-Fat Interaction Through Comparing 980 nm Diode Laser With 1064 nm Nd:YAG Laser. Research Article. J Skin Stem Cell 1(1):e17793. https://doi.org/10.17795/jssc17793
11. Mortazavi S, Mokhtari-Dizaji M (2023) Numerical study of high-intensity focused ultrasound (HIFU) in fat reduction. Skin Res Technol Jan 29(1):e13280. https://doi.org/10.1111/srt.13280
12. Passeron T, Olivier V, Duteil L, Desruelles F, Fontas E, Ortonne JP (2003) The new 940-nanometer diode laser: an effective treatment for leg venulectasia. J Am Acad Dermatol May 48(5):768–774. https://doi.org/10.1067/mjd.2003.191
13. Shen JC, Liang YY, Li W (2023) Quantitative simulation of photothermal effect in laser therapy of hypertrophic scar. Skin Res Technol 29(3):e13305. https://doi.org/10.1111/srt.13305
14. Suh DH, Choi JH, Lee SJ, Jeong KH, Song KY, Shin MK (2015) Comparative histometric analysis of the effects of high-intensity focused ultrasound and radiofrequency on skin. J Cosmet Laser Ther 17(5):230–236. https://doi.org/10.3109/14764172.2015.1022189
15. White WM, Makin IR, Barthe PG, Slayton MH, Gliklich RE (2007) Selective creation of thermal injury zones in the superficial musculoaponeurotic system using intense ultrasound therapy: a new target for noninvasive facial rejuvenation. Arch Facial Plast Surg 9. https://doi.org/10.1001/archfaci.9.1.22
16. Ye H, De S (2017) Thermal injury of skin and subcutaneous tissues: A review of experimental approaches and numerical models. Burns Aug 43(5):909–932. https://doi.org/10.1016/j.burns.2016.11.014
17. Yi K-H, Oh W, Kim H-M, Park H-J Is multiple wavelength diode laser for facial contouring safe? *Journal of Cosmetic Dermatology* n/a(n/a) https://doi.org/10.1111/jocd.16198

Publisher's note Springer Nature remains neutral with regard to jurisdictional claims in published maps and institutional affiliations.